# Increased Ocular Levels of MicroRNA-148a in Cases of Retinal Detachment Promote Epithelial–Mesenchymal Transition

Kei Takayama,[1] Hiroki Kaneko,[1] Shiang-Jyi Hwang,[1,2] Fuxiang Ye,[1,3] Akiko Higuchi,[1] Taichi Tsunekawa,[1] Toshiyuki Matsuura,[1] Takeshi Iwase,[1] Tetsu Asami,[1] Yasuki Ito,[1] Shinji Ueno,[1] Shunsuke Yasuda,[1] Norie Nonobe,[1] and Hiroko Terasaki[1]

[1]Department of Ophthalmology, Nagoya University Graduate School of Medicine, Nagoya, Japan
[2]Laboratory of Bell Research Center–Department of Obstetrics and Gynecology Collaborative Research, Nagoya University Graduate School of Medicine, Nagoya, Japan
[3]Department of Ophthalmology, Shanghai First People's Hospital, Shanghai Jiao Tong University School of Medicine, Shanghai, China

Correspondence: Hiroki Kaneko, Department of Ophthalmology, Nagoya University Graduate School of Medicine, 65 Tsurumai-cho, Showa-ku, Nagoya, 466-8550, Japan; h-kaneko@med.nagoya-u.ac.jp.

Submitted: November 17, 2015
Accepted: January 27, 2016

Citation: Takayama K, Kaneko H, Hwang S-J, et al. Increased ocular levels of microRNA-148a in cases of retinal detachment promote epithelial–mesenchymal transition. *Invest Ophthalmol Vis Sci.* 2016;57:2699–2705. DOI:10.1167/iovs.15-18660

**Purpose.** The purpose of this study was to determine microRNA expression in vitreous and subretinal fluid (SRF) samples from patients with retinal detachment (RD). The pathological importance of the identified microRNA transcript levels was analyzed in vitro.

**Methods.** Vitreous fluid was collected from 10 patients with macular hole (MH), vitreomacular traction syndrome (VMTS), or foveoschisis and from 11 patients with RD. Subretinal fluid was collected from 7 patients with RD. Of these, blood serum was collected in 4 patients. MicroRNA microarray profiling was performed to identify microRNA transcripts that were present in vitreous fluid, and more redundantly detected in SRF, of patients with RD, but not detected in control eyes. Western blotting and scratch assays were performed in ARPE-19 cells and primary human RPE cell lines transfected with microRNA to elucidate the effect of identified microRNA transcripts on epithelial–mesenchymal transition (EMT).

**Results.** MicroRNA microarray profiling revealed that hsa-miR-148a-3p was the most redundantly detected transcript in SRF and vitreous fluid from patients with RD, but not those with the other diseases. Expression levels of hsa-miR-148a-3p were higher in SRF samples than in blood serum samples in 3 out of 4 patients. Following hsa-miR-148a-3p mimic transfection, ARPE-19 and human RPE cells demonstrated increased expression of α-smooth muscle actin by Western blotting and increased migration ability during scratch assays.

**Conclusions.** The results of the present study indicate that hsa-miR-148a-3p was specifically detected in RD and promotes EMT in RPE.

Keywords: retinal detachment, proliferative vitreoretinopathy, microRNA, epithelial-mesenchymal transition

MicroRNAs are small noncoding RNA transcripts comprising 21 to 24 nucleotides that function in regulating various cellular processes through interfering with mRNA and protein levels.[1,2] Currently, more than 2000 microRNAs are reportedly involved in cell proliferation, differentiation, cell fate determination, signaling, organ development, and cellular responses to viral infection. MicroRNAs are reported to regulate approximately 50% of all cellular processes, including tumor formation.[3] MicroRNAs have been linked to a number of human diseases and have been studied as therapeutic targets or disease markers aiding clinical diagnoses.[4–6] In the eye, various microRNAs are thought to act on the retina or on the retinal pigment epithelium (RPE) and play important roles in neuroprotection and angiogenesis.[7–11]

Retinal detachment (RD), that is, detachment of the sensory retina from the RPE, is a leading cause of human blindness.[12] The most common clinically observed type of RD is rhegmatogenous RD (RRD), which is thought to be caused mainly by retinal breaks due to vitreous traction.[13] Scleral buckling and/or vitrectomy surgery are standard therapeutic methods for RRD.[14] During scleral buckling, subretinal fluid (SRF) is often aspirated through the drainage hole created in the sclera. During vitrectomy, vitreous fluid is removed using a vitrectomy cutter to reduce vitreous traction. Despite recent developments in surgical instruments and surgical skills that have allowed high rates of structural recovery following surgery,[15,16] major limitations of this approach remain. For instance, proliferative vitreoretinopathy (PVR), which develops in a proportion of patients with RRD, makes the surgical management more challenging.[17,18] Vitreous TGF-β levels are dysregulated in cases of PVR, and TGF-β-induced epithelial–mesenchymal transition (EMT) is involved in PVR pathogenesis.[19–21]

Although previous studies have examined the relevance of microRNAs in ophthalmic diseases, only a few have precisely evaluated microRNA profiles and functions in the vitreous fluid from eyes affected by RRD.[22–27] Moreover, no studies have compared microRNA profiles in vitreous fluid and SRF samples from patients with RRD. We hypothesized that specific microRNAs

may be increased in response to RRD, particularly in the SRF that is directly in contact with photoreceptors and the RPE, that is, the major sites of RRD-induced vision loss[28,29] and PVR pathogenesis.[17,30–33] Therefore, we examined and compared microRNA profiles in vitreous fluid and SRF from eyes with and without RRD. Furthermore, we examined the functional role in the RPE of a specific microRNA transcript found to be highly expressed in SRF.

## Materials and Methods

### Patients and Sample Collection

Seven SRF samples, 11 vitreous fluid samples, and 4 blood serum samples were collected from patients with RD. As controls, vitreous fluid was collected from 10 patients with macular hole (MH), vitreomacular traction syndrome (VMTS), or foveoschisis. Group 1 comprised patients with MH and VMTS or foveoschisis; group 2, patients with RD who had vitreous fluid collected; and group 3, patients with RD who had SRF collected. All vitreous samples were collected by dry vitrectomy at the beginning of vitrectomy surgery using a vitrectomy cutter before the initiation of infusions. All samples were immediately stored at −80°C until further experiments. Subretinal fluid was collected during scleral buckling surgery with surgical fields dried by surgical sponge-like materials (M.Q.A.; Inami, Tokyo, Japan) to avoid hemorrhagic contamination during SRF drainage. Peripheral blood was collected from patients who received scleral buckling surgery for the RD. Blood samples were subsequently centrifuged to isolate blood serum. Patients with severe systemic diseases, such as autoimmune diseases and cancer, were excluded. The present study adhered to the guidelines of the Declaration of Helsinki and was approved by the Nagoya University Hospital Ethics Review Board. Written informed consent was obtained from all included patients.

### RNA Isolation

Subretinal fluid, vitreous fluid, and blood serum samples were thawed on ice, centrifuged at 3000*g* for 5 minutes at 4°C to exclude cell debris, and stored prior to use in further experiments. Total RNA was extracted from supernatants using Qiagen miRNeasy Mini Kits (Qiagen GmbH, Hilden, Germany) according to the manufacturer's protocol. For normalization of sample-to-sample variation during RNA isolation procedures, 25 fmol synthetic *Caenorhabditis elegans* miRNA cel-miR-39 was added to total RNA samples, dissolved in RNase-free water, and stored at −80°C.

### MicroRNA Polymerase Chain Reaction (PCR) Array

Two, three, and three samples from groups 1, 2, and 3, respectively, were used for microRNA microarray. MicroRNA microarray profiling was performed using a miRCURY LNA Universal RT microRNA PCR System (Exiqon, Woburn, MA, USA) as previously described.[24] Single cDNA was synthesized by Universal cDNA Synthesis Kit II (Exiqon), mixed with miRCURY LNA ExiLENT SYBR Green master mix, and applied to Serum/Plasma Focus microRNA PCR panels. Data analyses were guided by miRCURY LNA Universal RT microRNA Ready-to-Use PCR panels using Exiqon GenEx software. Out of all microRNAs, hsa-miR-181a-5p was selected as the reference gene using the NormFinder algorithm. All other raw miR Cq values were standardized to hsa-miR-181a-5p levels.

### MicroRNA Real-Time Quantitative PCR (qPCR)

Quantitative PCR was performed to confirm the upregulation of candidate microRNA transcripts detected by microRNA microarray. For measurement of microRNA expression levels, specific primers against hsa-miR-148a-3p were used and its expression was quantified using TaqMan miR assays (Applied Biosystems, Foster City, CA, USA) according to the manufacturer's protocol using an MX3000p instrument (Stratagene, La Jolla, CA, USA). The number of miRNA copies was normalized using stably expressed RNU44 small nucleolar RNA. Cel-miR-39 was added, and its expression was measured to confirm the stability of experimental processes.

### MicroRNA Mimic Transfection

To confirm the effect of hsa-miR-148a-3p on human RPE cells, cells were transfected with 60 pmol hsa-miR-148a-3p mimic (Invitrogen, Carlsbad, CA, USA) prior to use in further in vitro experiments. ARPE-19 (American Type Culture Collection, Manassas, VA, USA) or primary human RPE (hRPE) cells (Lonza, Walkersville, MD, USA) were cultured in serum-free antibiotic-free Dulbecco's modified Eagle's medium (DMEM) premixed with Ham's F-12 (1:1 ratio; Sigma-Aldrich Corp., St. Louis, MO, USA) prior to incubation with Lipofectamine RNAiMAX Transfection Reagent and hsa-miR-148a-3p mimic for 48 hours. ARPE-19 or hRPE cells were also transfected with miRNA negative control (miR Ctrl) in the same manner and used as controls. Culture medium was then replaced with fresh medium containing 10% fetal bovine serum (FBS) and antibiotics and used in further experiments. Upregulation of hsa-miR-148a-3p in hRPE and ARPE-19 cells was confirmed before experiments (Supplementary Fig. S1).

### Western Blotting

Previous studies showed that TGF-β2, but not TGF-β1, was dominant in the retina and that it induces EMT in RPE.[34,35] Following hsa-miR-148a-3p mimic or miR Ctrl transfection and TGF-β2 (10 ng/mL) stimulation, hRPE cells were washed with PBS three times and then lysed in radioimmunoprecipitation assay (RIPA) buffer (Sigma-Aldrich Corp.) containing a protease inhibitor cocktail (Roche Diagnostics, Ltd., Mannheim, Germany). Protein lysates were obtained using the same procedure as above. Protein samples (20 μg) from human tissues or culture cells were run on 5% to 20% SDS precast gels (Wako, Tokyo, Japan) and transferred to polyvinylidene difluoride (PVDF) membranes using an iBlot blotting system (Invitrogen). Transferred membranes were washed in TBS-T (0.05M Tris, 0.138M NaCl, 0.0027M KCl, pH 8.0, 0.05% Tween 20; Sigma-Aldrich Corp.) and then blocked in 5% nonfat dry milk/TBS-T at room temperature (RT) for 2 hours. Membranes were then incubated with monoclonal anti-α-smooth muscle actin clone 1A4 antibody (α-SMA; 1:1000; Sigma-Aldrich Corp.) at 4°C overnight. Protein loading was assessed by immunoblotting using an anti–glyceraldehyde 3-phosphate dehydrogenase (GAPDH) antibody (1:3000; Cell Signaling Technology, Beverly, MA, USA). Membranes were then incubated with horseradish peroxidase (HRP)-linked secondary antibody (1:3000; Cell Signaling Technology) for 1 hour at RT. Signals were visualized with enhanced chemiluminescence (ECL plus; GE Healthcare, Piscataway, NJ, USA) and captured using ImageQuant LAS-4000 (GE Healthcare).

### Immunostaining

Zonula occludens-1 (ZO-1) was stained on hRPE cells using a technique similar to the one previously described.[36,37] In brief, after transfection with hsa-miR-148a-3p mimic or miR Ctrl, hRPE cells were maintained in medium with 1% FBS for 48 hours and then fixed with 100% methanol, stained with rabbit antibodies against ZO-1 (1:100; Invitrogen), and visualized with Alexa-594 (1:1000; Invitrogen) and 4′, 6-diamidino-2-phenyl-

TABLE. Characteristics of Patients From Whom Subretinal Fluid, Vitreous Fluid, and Blood Serum Were Collected

| Patient No. | Sample | PCR Array | RT-PCR miR-148a | Diseases | Age | Sex | Serum Collection |
|---|---|---|---|---|---|---|---|
| 1 | Vitreous fluid | Group 1-1 | | MH | 58 | F | |
| 2 | Vitreous fluid | Group 1-2 | | VMTS | 74 | M | |
| 3 | Vitreous fluid | | Not detected | MH | 56 | M | |
| 4 | Vitreous fluid | | Not detected | MH | 65 | M | |
| 5 | Vitreous fluid | | Not detected | VMTS | 70 | F | |
| 6 | Vitreous fluid | | Not detected | MH | 66 | F | |
| 7 | Vitreous fluid | | Not detected | VMTS | 74 | M | |
| 8 | Vitreous fluid | | Not detected | Foveoschisis | 77 | M | |
| 9 | Vitreous fluid | | Not detected | VMTS | 39 | M | |
| 10 | Vitreous fluid | | Not detected | MH | 71 | M | |
| 11 | Vitreous fluid | | Not detected | MH | 70 | M | |
| 12 | Vitreous fluid | Group 2-1 | | RD | 53 | F | |
| 13 | Vitreous fluid | Group 2-2 | | RD | 62 | M | |
| 14 | Vitreous fluid | Group 2-3 | | RD | 46 | M | |
| 15 | Vitreous fluid | | Detected | RD | 62 | M | |
| 16 | Vitreous fluid | | Detected | RD | 58 | M | |
| 17 | Vitreous fluid | | Detected | RD | 42 | M | |
| 18 | Vitreous fluid | | Detected | RD | 52 | M | |
| 19 | Vitreous fluid | | Not detected | RD | 81 | M | |
| 20 | Vitreous fluid | | Not detected | RD | 66 | M | |
| 21 | Vitreous fluid | | Not detected | RD | 53 | M | |
| 22 | Vitreous fluid | | Not detected | RD | 56 | F | |
| 23 | Subretinal fluid | Group 3-1 | | RD | 49 | F | |
| 24 | Subretinal fluid | Group 3-2 | | RD | 39 | F | |
| 25 | Subretinal fluid | Group 3-3 | | RD | 52 | M | |
| 26 | Subretinal fluid | | Detected | RD | 37 | M | + |
| 27 | Subretinal fluid | | Detected | RD | 54 | M | + |
| 28 | Subretinal fluid | | Detected | RD | 69 | M | + |
| 29 | Subretinal fluid | | Detected | RD | 21 | M | + |

MH, macular hole; VMTS, vitreomacular traction syndrome; RD, retinal detachment.

indole (DAPI; Invitrogen). Images were obtained using a scanning laser confocal microscope (A1-Rsi; Nikon, Tokyo, Japan).

### RPE Cell Migration Assay

After hsa-miR-148a-3p mimic or miR Ctrl transfection, ARPE-19 cells were replated. Cells were then serum starved for 24 hours before a single scratch wound was formed using a p20 pipette tip. The number of cells that had migrated into the wound space was assessed by light microscopy at 18 hours after scratch formation. Cell numbers were counted using built-in microscope software (FSX100; Olympus, Tokyo, Japan) and averaged. After hsa-miR-148a-3p mimic or miR Ctrl transfection, hRPE cells were replated on the 8-μm pore size culture inserts (Transwell; Costar, Badhoevedorp, The Netherlands). The Transwell membrane separates the upper and the lower chambers: 10% FBS-containing medium was added in the lower chamber, and serum-free medium was added in the upper chamber. After 24 hours, the cells that had migrated through the pores were stained, and the number of migrating cells from five vision fields was randomly counted under the microscope (BZ-9000; Keyence, Osaka, Japan) and averaged as $n = 1$. All experiments were performed at least three times.

### Statistics

Data were expressed as means ± standard errors of the mean (SEM; $n$ = number of samples). Values from control samples were defined as 100%, and percent change relative to controls was calculated for each sample. All comparisons were statistically analyzed using the Mann-Whitney $U$ test (unpaired samples). $P$ values $< 0.05$ were considered statistically significant.

## RESULTS

### Patients

Patient characteristics are summarized in the Table. Two out of 11 samples in group 1 (Nos. 1 and 2), 3 out of 11 samples in group 2 (Nos. 12, 13, and 14), and 3 out of 7 samples in group 3 (Nos. 23, 24, and 25) were used for microRNA PCR microarray. Vitreous samples were collected from patients in groups 1 and 2. Subretinal fluid was collected from patients in group 3. Groups 2 and 3 were composed of patients with RD. Group 1 was composed of patients with MH, VMTS, or foveoschisis. In group 3, four blood serum samples were collected in addition to SRF from the same patients (Nos. 26–29).

### Detection of hsa-miR-148a-3p

Based on the microRNA PCR array results, microRNAs detected in group 2 (Nos. 12, 13, and 14) and group 3 (Nos. 23, 24, and 25) but not group 1 (Nos. 1 and 2) were selected. Furthermore, microRNAs detected at high expression levels in group 3 (Nos. 23, 24, and 25) compared to group 2 (Nos. 12, 13, and 14) were listed depending on the ratio of the averaged relative expressions of group 3 (Nos. 23, 24, and 25) to group 2 (Nos. 12, 13, and 14). As a result, hsa-miR-148a-3p was found to be more highly expressed in SRF compared to vitreous fluid in patients with RD, but was not detected in vitreous fluid samples from patients with MH, VMTS, or foveoschisis (Fig. 1).

| | Group1 (G1) | Vitreous fluid from MH x 2 samples |
|---|---|---|
| | Group2 (G2) | Vitreous fluid from RD x 3 samples |
| | Group3 (G3) | Subretinal fluid from RD x 3 samples |

| | G2 | | | G3 | | | |
|---|---|---|---|---|---|---|---|
| miRname | Control G2-1 delta cq | Control G2-2 delta cq | Control G2-3 delta cq | Target G3-1 delta cq | Target G3-2 delta cq | Target G3-3 delta cq | Ratio |
| G1(−), G2(+) | delta cq in G2 | | | delta cq in G3 | | | G3/G2 ratio |
| hsa-miR-148a-3p | 4.4500 | 2.7600 | 2.0000 | −0.2800 | −0.0600 | −2.0500 | 3.8667 |
| hsa-miR-532-3p | 3.8700 | 2.7900 | 3.0900 | −0.7100 | 1.9200 | −1.0600 | 3.2000 |
| hsa-miR-99b-5p | 1.9700 | 2.2800 | 1.4400 | −0.8600 | −0.2500 | −1.2800 | 2.6933 |
| hsa-miR-186-5p | 3.8100 | 1.2500 | 0.6200 | −0.2100 | −0.8200 | −0.7200 | 2.4767 |
| hsa-miR-484 | 2.9700 | 1.3500 | 1.3600 | −0.2900 | −0.9800 | 0.0700 | 2.2933 |
| hsa-let-7e-5p | 3.2300 | 4.2000 | 6.4800 | 2.7300 | 2.6100 | 2.0700 | 2.1667 |
| hsa-miR-185-5p | 3.5000 | 1.0700 | −1.6800 | −0.7000 | −1.1500 | −1.7600 | 2.1667 |
| hsa-miR-30b-5p | 1.4000 | 3.1600 | 2.0400 | 0.5300 | −0.0100 | −0.4000 | 2.1600 |
| hsa-miR-101-3p | 0.2000 | 1.1100 | −1.6500 | −1.8100 | −1.7700 | −3.2300 | 2.1567 |
| hsa-miR-660-5p | 0.6300 | 0.8700 | 0.4200 | −1.1800 | −0.7400 | −2.4600 | 2.1000 |
| hsa-miR-151a-3p | 3.6500 | 5.4700 | 3.6000 | 2.1500 | 2.8200 | 1.7700 | 1.9933 |
| hsa-miR-148b-3p | 1.8800 | 0.7500 | 0.1300 | −0.5400 | −0.0600 | −2.2400 | 1.8667 |
| hsa-miR-152 | 1.7900 | 0.4600 | 1.8600 | −0.0900 | −0.2700 | −1.0400 | 1.8367 |
| hsa-miR-27a-3p | 3.2100 | 0.5600 | 3.6100 | 0.5500 | 2.7100 | −0.7400 | 1.6200 |
| hsa-miR-142-3p | 4.2900 | 1.9900 | 1.3000 | 0.9900 | 1.7000 | 0.1200 | 1.5900 |
| hsa-miR-125a-5p | 3.5000 | 0.8500 | 2.0800 | 0.1800 | 1.3100 | 0.6500 | 1.4300 |
| hsa-miR-194-5p | 4.3700 | 4.9800 | 1.0500 | 2.2900 | 2.2900 | 1.7900 | 1.3433 |
| hsa-miR-140-3p | 1.0900 | 0.0800 | −1.0300 | −0.9700 | −1.3100 | −1.1900 | 1.2033 |
| hsa-miR-140-5p | 5.6900 | 1.0800 | 2.3400 | 2.0000 | 2.8500 | 0.8400 | 1.1400 |
| hsa-miR-425-5p | 2.0700 | 0.1900 | −1.2100 | −1.2500 | −0.3300 | −0.6300 | 1.0867 |
| hsa-miR-590-5p | 2.7900 | 6.6400 | 2.2100 | 3.4900 | 3.1400 | 1.8000 | 1.0700 |
| hsa-miR-30c-5p | 1.9400 | 3.3000 | 2.0600 | 1.2700 | 1.9400 | 0.9000 | 1.0633 |
| hsa-miR-502-3p | 2.2900 | 1.3100 | 2.6400 | 1.0400 | 2.3400 | −0.1100 | 0.9900 |
| hsa-miR-30e-3p | 5.3000 | 2.9800 | 5.0100 | 4.2100 | 3.3100 | 2.9700 | 0.9333 |
| hsa-miR-652-3p | 1.2200 | −0.2100 | −0.9100 | −0.8100 | 0.0600 | −1.7900 | 0.8800 |
| hsa-miR-33a-5p | 5.2200 | 4.3300 | 4.0400 | 4.6300 | 4.5500 | 2.2100 | 0.7333 |
| hsa-miR-30d-5p | 3.8200 | 2.7000 | 4.3300 | 1.8500 | 4.8700 | 2.0100 | 0.7067 |
| hsa-miR-15b-5p | 3.5100 | 4.5900 | 0.9300 | 2.7900 | 2.9400 | 1.2000 | 0.7000 |
| hsa-miR-378a-3p | 1.2000 | −0.4400 | 0.6400 | −0.2300 | 0.0100 | −0.4800 | 0.7000 |
| hsa-miR-95 | 5.9000 | 3.7000 | 3.5800 | 3.3500 | 5.0100 | 4.0500 | 0.2567 |
| hsa-miR-425-3p | 5.2900 | 3.9300 | 2.6000 | 4.2100 | 4.0400 | 3.0800 | 0.1633 |
| hsa-miR-151a-5p | 1.8400 | 0.0100 | 0.8300 | 0.9700 | 1.2500 | 0.2500 | 0.0700 |
| hsa-miR-421 | 3.7300 | 2.2300 | 6.4300 | 4.8900 | 3.7200 | 4.1800 | −0.1333 |
| hsa-miR-107 | 1.9300 | 1.3500 | −1.6100 | 0.8200 | 1.3900 | −0.0900 | −0.1500 |
| hsa-let-7f-5p | 3.6400 | 3.4900 | 1.4900 | 2.9500 | 4.0700 | 2.4800 | −0.2933 |
| hsa-let-7d-5p | 2.6100 | 3.0500 | 0.8200 | 2.2800 | 4.0500 | 1.9800 | −0.6100 |
| hsa-miR-505-3p | 4.0300 | 2.6700 | 3.3400 | 4.2600 | 4.0300 | 3.7900 | −0.6800 |
| hsa-miR-142-5p | 2.9900 | 3.3400 | 1.8600 | 3.0100 | 4.9800 | 2.7400 | −0.8467 |
| hsa-miR-103a-3p | −0.3900 | −0.2400 | −3.0200 | −0.1700 | 0.7600 | −1.4600 | −0.9267 |
| hsa-miR-150-5p | 1.1600 | 4.8800 | −0.4600 | 1.0900 | 4.8300 | 2.5800 | −0.9733 |
| hsa-miR-197-3p | 2.5600 | −0.8600 | 3.2200 | 2.9100 | 3.2600 | 1.9200 | −1.0566667 |
| hsa-miR-26b-5p | 4.3400 | 2.8500 | 2.7700 | 4.5000 | 5.9500 | 2.7900 | −1.0933333 |

**Figure 1.** MicroRNA microarray results from subretinal and vitreous fluid samples from patients with macular hole (MH) or retinal detachment (RD). Out of all candidate microRNAs detected in vitreous fluid from patients with RD (but not patients with MH), hsa-miR-148a-3p was found to be the most redundantly expressed microRNA in subretinal fluid samples. Heat map colors on the *right side* indicate the G3/G2 expression ratio. G1, vitreous fluid from MH; G2, vitreous fluid from RD; G3, subretinal fluid from RD.

To confirm the specificity of hsa-miR-148a-3p detection, qPCR was performed with additional samples. Hsa-miR-148a-3p was not detected in samples from any of the 11 patients in group 1, but was detected in 7 out of 11 samples in group 2 and all 7 samples in group 3 (Table). As hsa-miR-148a-3p has been reported to be present in blood samples,[38,39] frequent detection of hsa-miR-148a-3p in group 3 may have been due to blood contamination. Verifying this possibility, hsa-miR-148a-3p was found to be detected in both blood and SRF samples in 4 patients in group 3. Quantitative PCR demonstrated higher relative expression of hsa-miR-148a-3p in SRF compared to blood serum in 3 out of 4 patients in group 3 (Fig. 2). These findings indicate that the detection of hsa-miR-148a-3p in group 3 was not due to contamination by blood serum.

## Changes in α-SMA and ZO-1 Expression Following hsa-miR-148a-3p Transfection

In order to elucidate the function of hsa-miR-148a-3p in vitreous fluid and SRF from patients with RD, we evaluated the contribution of hsa-miR-148a-3p to PVR pathogenesis. Epithe-

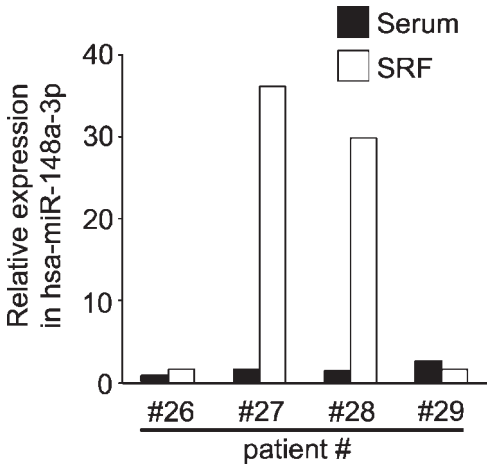


**Figure 2.** Relative expression of hsa-miR-148a-3p in blood serum and subretinal fluid samples from the same patients. Expression levels of hsa-miR-148a-3p were higher in subretinal fluid compared to blood serum samples in 3 out of 4 patients. Patient numbers correspond to those presented in the Table.

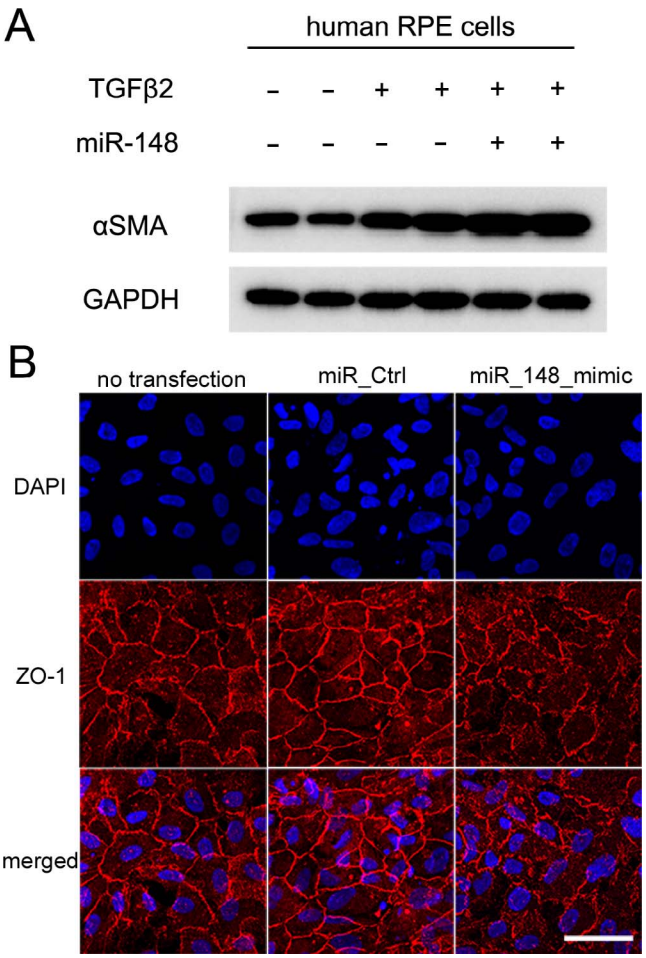


**Figure 3.** Western blot images from primary human RPE (hRPE) cells transfected with hsa-miR-148-3p. (**A**) α-SMA levels were increased in response to TGF-β2 stimulation (*middle two lanes*), and further increased following incubation with hsa-miR-148-3p (*right two lanes*). GAPDH was used as a loading control. (**B**) After hsa-miR-148-3p transfection, hRPE showed reduced expression of zonula occludens-1 (ZO-1) compared to hRPE transfected with control microRNA (miR Ctrl). *Scale bar*: 50 μm.

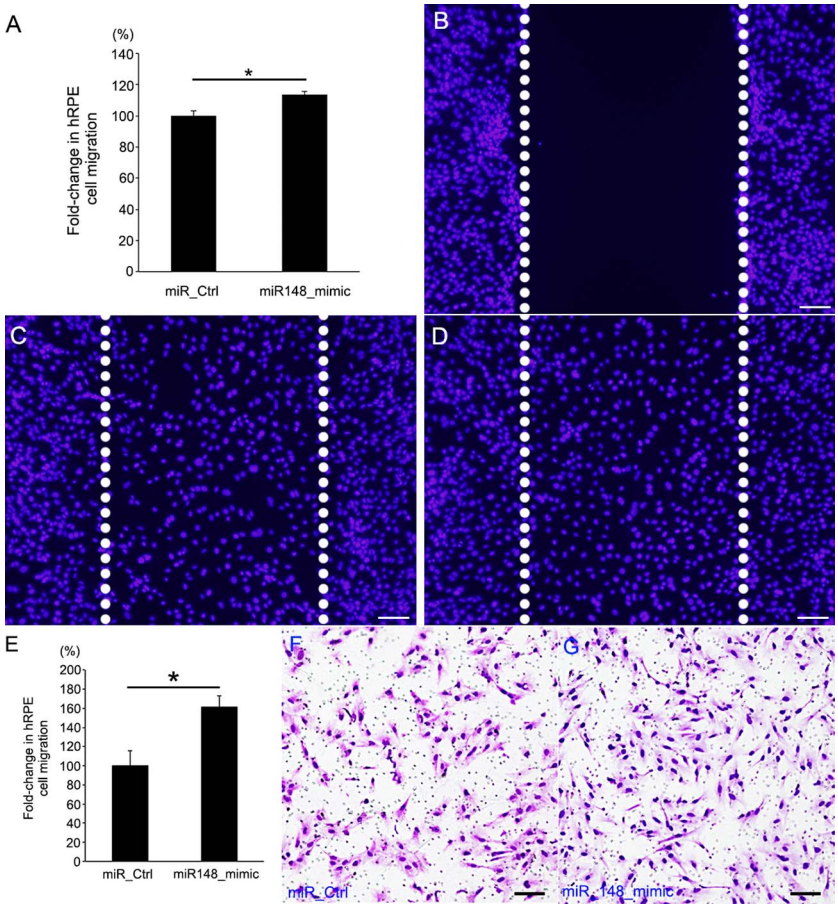


**Figure 4.** Effect of hsa-miR-148-3p on ARPE-19 and hRPE cell migration. (**A**) The number of migrating ARPE-19 cells was significantly higher in cells transfected with hsa-miR-148a-3p mimic compared to cells transfected with miR Ctrl. (**B**) Images of ARPE-19 cells immediately following scratch formation. (**C**, **D**) Representative images of ARPE-19 cells transfected with miR Ctrl (**C**) and hsa-miR-148a-3p mimic (**D**). Photographs were captured at 18-hour scratch formation. *Dashed lines* delineate scratched areas. (**E**) The number of migrating hRPE cells through the Transwell membrane was significantly higher in cells transfected with hsa-miR-148a-3p mimic than in cells transfected with miR Ctrl. (**F**, **G**) Representative images of hRPE cells transfected with miR Ctrl (**F**) and hsa-miR-148a-3p mimic (**G**). Photographs were captured at 24 hours after plating cells on Transwell membranes. *Scale bars*: 100 μm.

lial–mesenchymal transition has been posited as a trigger for PVR following RD.[19,40] Further, α-SMA expression is reportedly increased in RPE cells undergoing EMT. We examined α-SMA expression in hRPE cells following transfection with hsa-miR-148a-3p mimic and miR Ctrl. Human RPE cell viability was not significantly changed after hsa-miR-148a-3p transfection (Supplementary Fig. S2). Interestingly, α-SMA expression was found to be upregulated in hRPE cells transfected with hsa-miR-148a-3p mimic compared to cells transfected with miR Ctrl (Fig. 3A). In addition, ZO-1 immunostaining showed that hsa-miR-148a-3p mimic transfection induced reduction of ZO-1 expression and disruption of RPE morphology, whereas miR Ctrl did not (Fig. 3B).

### Changes in Migration Ability Following hsa-miR-148a-3p Transfection

To further elucidate the role of hsa-miR-148a-3p in RD, we studied the migration ability of ARPE-19 cells and hRPE cells with and without the transfection of hsa-miR-148a-3p (Fig. 4). In scratch assay, compared to ARPE-19 cells transfected with hsa-miR-148a-3p mimic (1.00 ± 0.03, $n = 43$), those transfected with hsa-miR-148a-3p mimic demonstrated significantly increased numbers of migrating cells (1.13 ± 0.02; $n = 43$; $P = 0.0005$, Figs. 4A–D). Consistent with the results from the scratch assay, Transwell migration assay showed that compared to hRPE cells transfected with hsa-miR-148a-3p mimic (1.00 ± 0.15, $n = 6$), those transfected with hsa-miR-148a-3p mimic demonstrated significantly increased numbers of migrating cells (1.61 ± 0.12; $n = 6$; $P = 0.0039$, Figs. 4E–G). These results indicate that hsa-miR-148a-3p detected vitreous fluid and that SRF from eyes with RRD promotes EMT in RPE cells, which possibly plays a role in PVR pathogenesis.

## Discussion

Recently, there has been accumulating evidence of a biological relationship between microRNAs and ocular diseases. For instance, miR-155 has been shown to promote the expansion of pathogenic Th17 cells, which mediate experimental uveitis[41]; intravitreal miR-21 and miR-146 have been demonstrated as tumor markers of uveal melanoma[26]; and intravitreal miR-146 has been demonstrated to control retinal inflammation in diabetic retinitis.[23] Further, the expression levels of microRNA transcripts have been compared between patients with proliferative diabetic retinopathy and patients with MH.[24] To the best of our knowledge, comparisons of microRNA transcript levels in vitreous fluid samples from eyes with and without RRD have yet to be reported, and no studies have

performed microRNA profile comparisons of SRF samples. In the present study, hsa-miR-148a-3p was detected in vitreous fluid and SRF samples from RD eyes, with the expression levels of hsa-miR-148a-3p found to higher in SRF compared to vitreous fluid samples. The administration of miR-148a resulted in the upregulation of α-SMA expression in hRPE cells and increased migration ability of both hRPE cells and ARPE-19 cells, which represent the induction of EMT. One of the limitation and difficulties in measuring microRNAs in the ocular fluids is the setting-up protocol for precisely detecting low-abundance RNAs, for example, microRNAs. For instance, spiking in the control RNA after RNA extraction is sometimes used and may control for cDNA and qPCR differences between samples. However, it does not control for RNA extraction efficiency in many situations. Nevertheless, limited sample volumes disable researchers with respect to finding the best experimental condition. Further accumulation of knowledge will enable us to find the solution for this problem. On the other hand, it is very interesting that even under the different experiments with different references, hsa-miR-148a-3p abundance was confirmed by both PCR array and qPCR using two different reference genes.

There have been no reports describing a relationship between miR-148a and intraocular diseases other than RD; however, miR-148a has been reported to contribute to the pathogenesis of a number of extraocular diseases. Yuan et al.[42] reported that miR-148a was upregulated in hepatocellular carcinoma cells and promoted cell proliferation, cell cycle progression, cell migration, anchorage-independent growth in soft agar, and subcutaneous tumor formation. Increased miR-148a expression levels in aortic valve interstitial cells have been shown to decrease nuclear factor kappa-light-chain-enhancer of activated B (NF-κB) cell signaling and NF-κB target gene expression, and promote valvular inflammation and distension.[43] In adipocytes, miR-148a increased adipogenesis and suppressed *Wnt1* expression, an endogenous inhibitor of adipogenesis. Ectopic expression of miR-148a reportedly accelerates the differentiation of mesenchymal stem cells through Wnt signaling.[44] Further, cells expressing miR-148a have been shown to produce greater amounts of proteoglycans and collagen, in particular type II collagen, with proteoglycan and collagen secretion into culture medium shown to be inhibited, but total collagen production increased, by miR-148a.[45] These corroborating studies indicate that miR-148a has multifunction roles depending on cellular conditions. In the present study, miR-148a upregulation was found to promote EMT in RPE cells. However, we were unable to elucidate the detailed mechanisms underlying the promotion of EMT by miR-148a. Further studies are required to fully elucidate the biological mechanisms underlying the promotion of EMT by miR-148a. More importantly, we did not show the clinical relationship of hsa-miR-148a upregulation in the eyes and pathogenesis of PVR. To elucidate the clinical importance of abundant hsa-miR-148a expression in the eyes, it is necessary to collect vitreous fluids from eyes with PVR and examine the expression of hsa-miR-148a. In addition, it would be interesting to measure hsa-miR-148a expression in the vitreous fluid and SRF of RD eyes in each case and examine the correlation of clinical severity of RD as a predictive factor of PVR.

In conclusion, hsa-miR-148a is increased in vitreous fluid and SRF of eyes affected by RRD and promotes EMT in RPE cells.

## Acknowledgments

The authors thank Reona Kimoto and Chisato Ishizuka for technical assistance.

Supported in part by Grants-in-Aid for Scientific Research B (15H04994, HT) and for Young Scientists A (25713056, HK) from the Japan Society for the Promotion of Science, Takeda Medical Research Foundation (HK), Takeda Science Foundation (HK), Japan Intractable Diseases Research Foundation (HK), Yokoyama Foundation for Clinical Pharmacology (YRY1411, HK), and The Uehara Memorial Foundation (HK), Hori Science and Arts Foundation (FY), and Mishima Saiichi Memorial Ophthalmic Research International Foundation (FY).

Disclosure: **K. Takayama**, None; **H. Kaneko**, None; **S.-J. Hwang**, None; **F. Ye**, None; **A. Higuchi**, None; **T. Tsunekawa**, None; **T. Matsuura**, None; **T. Iwase**, None; **T. Asami**, None; **Y. Ito**, None; **S. Ueno**, None; **S. Yasuda**, None; **N. Nonobe**, None; **H. Terasaki**, None

## References

1. Ambros V. microRNAs: tiny regulators with great potential. *Cell*. 2001;107:823–826.
2. Huang Y, Shen XJ, Zou Q, Wang SP, Tang SM, Zhang GZ. Biological functions of microRNAs: a review. *J Physiol Biochem*. 2011;67:129–139.
3. Krol J, Loedige I, Filipowicz W. The widespread regulation of microRNA biogenesis, function and decay. *Nat Rev Genet*. 2010;11:597–610.
4. Allegra A, Alonci A, Campo S, et al. Circulating microRNAs: new biomarkers in diagnosis, prognosis and treatment of cancer (review). *Int J Oncol*. 2012;41:1897–1912.
5. Taft RJ, Pang KC, Mercer TR, Dinger M, Mattick JS. Non-coding RNAs: regulators of disease. *J Pathol*. 2010;220:126–139.
6. Tomankova T, Petrek M, Gallo J, Kriegova E. MicroRNAs: emerging regulators of immune-mediated diseases. *Scand J Immunol*. 2012;75:129–141.
7. Cao Y, Feng B, Chen S, Chu Y, Chakrabarti S. Mechanisms of endothelial to mesenchymal transition in the retina in diabetes. *Invest Ophthalmol Vis Sci*. 2014;55:7321–7331.
8. Chung SH, Gillies M, Sugiyama Y, Zhu L, Lee S-R, Shen W. Profiling of MicroRNAs involved in retinal degeneration caused by selective müller cell ablation. *PLoS One*. 2015;10: e0118949.
9. Takahashi Y, Chen Q, Rajala RV, Ma JX. MicroRNA-184 modulates canonical Wnt signaling through the regulation of frizzled-7 expression in the retina with ischemia-induced neovascularization. *FEBS Lett*. 2015;589:1143–1149.
10. Ye EA, Steinle JJ. miR-15b/16 protects primary human retinal microvascular endothelial cells against hyperglycemia-induced increases in tumor necrosis factor alpha and suppressor of cytokine signaling 3. *J Neuroinflammation*. 2015;12:44.
11. Yoon C, Kim D, Kim S, et al. MiR-9 regulates the post-transcriptional level of VEGF165a by targeting SRPK-1 in ARPE-19 cells. *Graefes Arch Clin Exp Ophthalmol*. 2014;252: 1369–1376.
12. Bourne RR, Stevens GA, White RA, et al. Causes of vision loss worldwide, 1990-2010: a systematic analysis. *Lancet Glob Health*. 2013;1:e339–e349.
13. Colucciello M. Rhegmatogenous retinal detachment. *Phys Sportsmed*. 2009;37:59–65.
14. Lane JI, Watson RE Jr, Witte RJ, McCannel CA. Retinal detachment: imaging of surgical treatments and complications. *Radiographics*. 2003;23:983–994.
15. Kreissig I. Surgical techniques for repair of primary retinal detachment: part I. Review of their development during the last 80 years. *Folia Med (Plovdiv)*. 2009;51:5–11.
16. Sodhi A, Leung LS, Do DV, Gower EW, Schein OD, Handa JT. Recent trends in the management of rhegmatogenous retinal detachment. *Surv Ophthalmol*. 2008;53:50–67.

17. Pastor JC. Proliferative vitreoretinopathy: an overview. *Surv Ophthalmol*. 1998;43:3–18.
18. Kirchhof B. Strategies to influence PVR development. *Graefes Arch Clin Exp Ophthalmol*. 2004;242:699–703.
19. Hoerster R, Muether PS, Vierkotten S, Hermann MM, Kirchhof B, Fauser S. Upregulation of TGF-ss1 in experimental proliferative vitreoretinopathy is accompanied by epithelial to mesenchymal transition. *Graefes Arch Clin Exp Ophthalmol*. 2014;252:11–16.
20. Cao Y, Feng B, Chen S, Chu Y, Chakrabarti S. Mechanisms of endothelial to mesenchymal transition in the retina in diabetes. *Invest Ophthalmol Vis Sci*. 2014;55:7321–7331.
21. Winkler J, Hoerauf H. TGF-ss and RPE-derived cells in taut subretinal strands from patients with proliferative vitreoretinopathy. *Eur J Ophthalmol*. 2011;21:422–426.
22. Escobar T, Yu C-R, Muljo SA, Egwuagu CE. STAT3 activates miR-155 in Th17 cells and acts in concert to promote experimental autoimmune uveitis. *Invest Ophthalmol Vis Sci*. 2013;54:4017–4025.
23. Fulzele S, El-Sherbini A, Ahmad S, et al. MicroRNA-146b-3p regulates retinal inflammation by suppressing adenosine deaminase-2 in diabetes. *Biomed Res Int*. 2015;2015:846501.
24. Hirota K, Keino H, Inoue M, Ishida H, Hirakata A. Comparisons of microRNA expression profiles in vitreous humor between eyes with macular hole and eyes with proliferative diabetic retinopathy. *Graefes Arch Clin Exp Ophthalmol*. 2015;253:335–342.
25. Odriozola A, Riancho JA, de la Vega R, et al. miRNA analysis in vitreous humor to determine the time of death: a proof-of-concept pilot study. *Int J Legal Med*. 2013;127:573–578.
26. Ragusa M, Barbagallo C, Statello L, et al. miRNA profiling in vitreous humor, vitreal exosomes and serum from uveal melanoma patients: pathological and diagnostic implications. *Cancer Biol Ther*. 2015;16:1387–1396.
27. Ragusa M, Caltabiano R, Russo A, et al. MicroRNAs in vitreous humor from patients with ocular diseases. *Mol Vis*. 2013;19:430.
28. Quintyn JC, Brasseur G. Subretinal fluid in primary rhegmatogenous retinal detachment: physiopathology and composition. *Surv Ophthalmol*. 2004;49:96–108.
29. Veckeneer M, Derycke L, Lindstedt EW, et al. Persistent subretinal fluid after surgery for rhegmatogenous retinal detachment: hypothesis and review. *Graefes Arch Clin Exp Ophthalmol*. 2012;250:795–802.
30. Charteris DG, Sethi CS, Lewis GP, Fisher SK. Proliferative vitreoretinopathy-developments in adjunctive treatment and retinal pathology. *Eye (Lond)*. 2002;16:369–374.
31. Williamson TH, Laidlaw DA, Doyle E. Aggregations of retinal pigment epithelial cells on inferior retinal blood vessels, a clinical sign of early proliferative vitreoretinopathy. *Clin Experiment Ophthalmol*. 2008;36:744–747.
32. Qiu S, Jiang Z, Huang Z, et al. Migration of retinal pigment epithelium cells is regulated by protein kinase Calpha in vitro. *Invest Ophthalmol Vis Sci*. 2013;54:7082–7090.
33. Feist RM Jr, King JL, Morris R, Witherspoon CD, Guidry C. Myofibroblast and extracellular matrix origins in proliferative vitreoretinopathy. *Graefes Arch Clin Exp Ophthalmol*. 2014;252:347–357.
34. Connor TB Jr, Roberts AB, Sporn MB, et al. Correlation of fibrosis and transforming growth factor-beta type 2 levels in the eye. *J Clin Invest*. 1989;83:1661–1666.
35. Sugioka K, Kodama A, Okada K, et al. TGF-beta2 promotes RPE cell invasion into a collagen gel by mediating urokinase-type plasminogen activator (uPA) expression. *Exp Eye Res*. 2013;115:13–21.
36. Kaneko H, Dridi S, Tarallo V, et al. DICER1 deficit induces Alu RNA toxicity in age-related macular degeneration. *Nature*. 2011;471:325–330.
37. Ijima R, Kaneko H, Ye F, et al. Interleukin-18 induces retinal pigment epithelium degeneration in mice. *Invest Ophthalmol Vis Sci*. 2014;55:6673–6678.
38. Li L, Chen YY, Li SQ, Huang C, Qin YZ. Expression of miR-148/152 family as potential biomarkers in non-small-cell lung cancer. *Med Sci Monit*. 2015;21:1155–1161.
39. Yang JS, Li BJ, Lu HW, et al. Serum miR-152, miR-148a, miR-148b, and miR-21 as novel biomarkers in non-small cell lung cancer screening. *Tumour Biol*. 2015;36:3035–3042.
40. Chen Z, Shao Y, Li X. The roles of signaling pathways in epithelial-to-mesenchymal transition of PVR. *Mol Vis*. 2015;21:706–710.
41. Escobar T, Yu CR, Muljo SA, Egwuagu CE. STAT3 activates miR-155 in Th17 cells and acts in concert to promote experimental autoimmune uveitis. *Invest Ophthalmol Vis Sci*. 2013;54:4017–4025.
42. Yuan K, Lian Z, Sun B, Clayton MM, Ng IO, Feitelson MA. Role of miR-148a in hepatitis B associated hepatocellular carcinoma. *PLoS One*. 2012;7:e35331.
43. Patel V, Carrion K, Hollands A, et al. The stretch responsive microRNA miR-148a-3p is a novel repressor of IKBKB, NF-kappaB signaling, and inflammatory gene expression in human aortic valve cells. *FASEB J*. 2015;29:1859–1868.
44. Shi C, Zhang M, Tong M, et al. miR-148a is associated with obesity and modulates adipocyte differentiation of mesenchymal stem cells through wnt signaling. *Sci Rep*. 2015;5:9930.
45. Vonk LA, Kragten AH, Dhert WJ, Saris DB, Creemers LB. Overexpression of hsa-miR-148a promotes cartilage production and inhibits cartilage degradation by osteoarthritic chondrocytes. *Osteoarthritis Cartilage*. 2014;22:145–153.

Investigative Ophthalmology & Visual Science